Title
MULTI-REGGE APPROACH TO HIGH ENERGY PRODUCTION PROCESSES

Authors
Bali, Naren F.
Chew, Geoffrey F.
Pignotti, Alberto.

Publication Date
1967-12-01

University of California

Ernest O. Lawrence Radiation Laboratory

MULTI-REGGE APPROACH
TO HIGH ENERGY PRODUCTION PROCESSES

Naren F. Bali, Geoffrey F. Chew, and Alberto Pignotti

December 1967

Submitted to Topical Conference on
High Energy Collisions of Hadrons
CERN, Geneva, Switzerland
January 15-18, 1968

UCRL-17980
Preprint

UNIVERSITY OF CALIFORNIA

Lawrence Radiation Laboratory
Berkeley, California

AEC Contract No. W-7405-eng-48

MULTI-REGGE APPROACH TO HIGH ENERGY PRODUCTION PROCESSES

Naren F. Bali, Geoffrey F. Chew, and Alberto Pignotti

December 1967

MULTI - REGGE APPROACH TO HIGH ENERGY PRODUCTION PROCESSES

Naren F. Bali,

Department of Physics, University of Washington,
Seattle, Washington, U. S. A.

and

Geoffrey F. Chew,

Department of Physics and Lawrence Radiation Laboratory,
University of California,
Berkeley, California, U. S. A.

and

Alberto Pignotti,

Lawrence Radiation Laboratory, University of California,
Berkeley, California, U. S. A.

December 1967

1. INTRODUCTION

In recent years the experimental study of strong interactions has concentrated on discovering and determining the quantum numbers of an increasing family of (mostly unstable) particles. As a consequence, it has often happened that the attention of physicists was devoted to a comparatively small part of the total cross section. Furthermore, because the coupling of the more massive particles to the few available primary particles decreases as the mass increases, the identification of the new particles becomes harder, and they account for an even smaller part of the almost constant total cross section.

This state of affairs is a consequence of the attractive simplicity of the interpretation of unstable particle states, described by a small number of parameters. On the other hand, it is often not even clear what variables to use in the case of production of several uncorrelated particles. Our concern here is with the latter aspect of hadronic processes - especially in the high energy region. We first summarize some recent work on the subject[1), 2)] and then propose a detailed model for production processes. We show as an example a preliminary calculation for the proton-proton case which, in spite of its limitations, illustrates certain basic features of the model.

2. TOLLER VARIABLES

2.1 Introduction

The extension of the Regge pole idea to the multi-Regge case, represented diagrammatically in Fig. 1, was considered by many authors in the past years[3)-18)]. We approach the problem from a slightly different angle, by generalising Toller's technique[19)] to the multi-Regge case. The advantage of this approach is

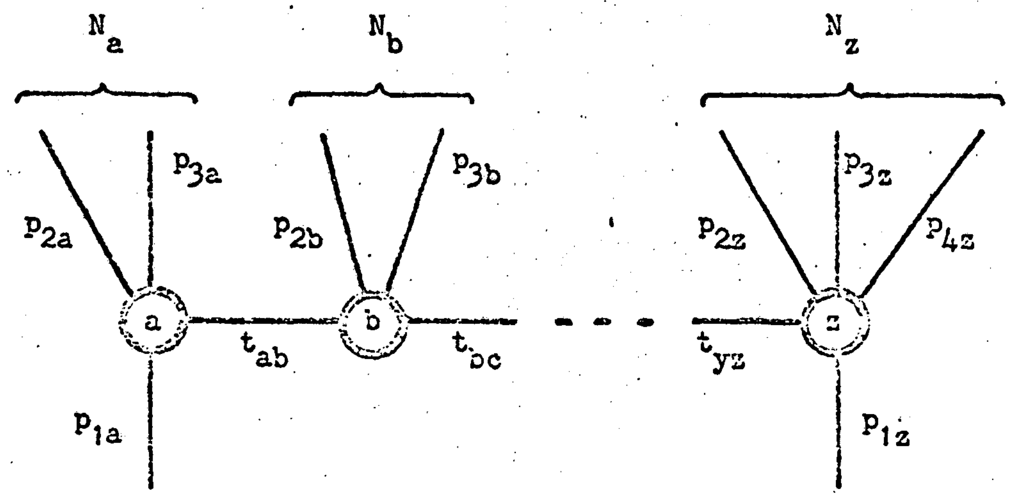

Fig. 1

twofold: it provides a natural set of variables (Toller variables) for the description of a multi-peripheral process, and makes it possible to formulate the multi-Regge-pole hypothesis without appeal to analytic continuation from the crossed channels.

2.2 The Partial Wave Expansion

Let us start by a familiar example: suppose we want to describe the amplitude for the process with two initial and three final spinless particles shown in Fig. 2, at a fixed

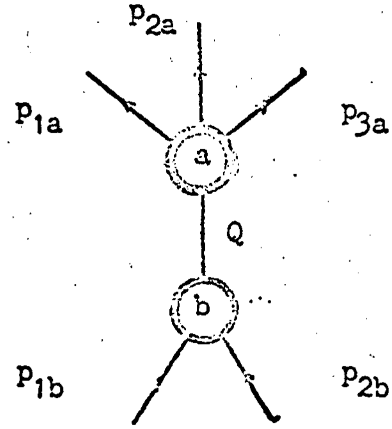

Fig. 2

value of the total energy-momentum four vector Q. We choose a frame "b" in which $\underset{\sim}{Q} = 0$ and $\underset{\sim}{p}_{1b}$ and $\underset{\sim}{p}_{2b}$ point in the z direction, and a second frame "a" in which again $\underset{\sim}{Q} = 0$ and now $\underset{\sim}{p}_{1a}$ points in the z direction, while $\underset{\sim}{p}_{2a}$ and $\underset{\sim}{p}_{3a}$ lie in the y-z plane. Of course, the complete description of the final state in frame "a" requires two more degrees of freedom corresponding to different possible shapes of the triangle formed by $\underset{\sim}{p}_{1a}$, $\underset{\sim}{p}_{2a}$, and $\underset{\sim}{p}_{3a}$. (Once the shape of the triangle is given, the size is determined by energy conservation). We call these two degrees of freedom "internal variables" of cluster "a", and denote them by V_a. In general, if there are $N_a + 1$ particles attached to cluster "a", the number of corresponding internal variables is $3 N_a - 4$.

In our two-to-three particles example we have up to now introduced three variables: Q^2 and V_a, and two different frames, "a" and "b". In both these frames we have

$$\underset{\sim}{Q} = 0. \qquad (2.2.1)$$

We can now complete the description of the process by specifying the relative orientation of frames "a" and "b". In order to satisfy Eq. (2.2.1) in both frames, this is just a rotation, or, in a somewhat more difficult language, an element of the little group of the homogeneous Lorentz group with respect to the four-vector Q. We parametrize this transformation by three Euler angles α, θ and β, which we designate collectively by g. Because the initial state is a two-particles state, it defines a direction but not a plane, and the amplitude is independent of β. In the general case in which more than two particles are attached to cluster "b", not only does the amplitude depend on β, but also on $3N_b - 4$ internal variables of cluster "b". Thus, we can denote in full generality the amplitude as

$$f(V_a, g, Q^2, V_b).$$

Using a completeness theorem, this amplitude can be expanded as a sum over projections on the unitary irreducible representations of the rotation group. This is just the well-known partial-wave expansion.

2.3 The Expansion at Fixed Momentum Transfer

Now consider the case in which $Q^2 = t < 0$, and we are in the physical region for a process in which p_{1b} and $-p_{1a}$ are are the four-momenta of the incoming particles. Toller's analysis consists in choosing again two frames, "a" and "b", in both of which Q takes the form

$$Q = (0, 0, 0, \sqrt{-t}). \tag{2.3.1}$$

The relative orientation of the two frames is now given by an element of the three-dimensional Lorentz group. We parametrize it by a rotation around the z axis of angle ν, a boost in the x direction of parameter ζ, and a new rotation around the z axis of angle μ. The expansion has now to be done over projections on the unitary irreducible representations of the three-dimensional Lorentz group which run in the complex j plane along the line $\mathrm{Re}\, j = -\frac{1}{2}$. Toller[19] has shown how, by shifting this contour, one picks up leading contributions of the Regge pole type for the asymptotic behavior in the energy.

2.4 Definition of the Toller Variables

Now we go to the multi-Regge case of Fig. 1, in which we fix a number of invariant momentum transfers, t_{ab}, t_{bc}, ..., t_{yz}, thereby defining a given grouping of the final particles in various clusters. We consider for simplicity the spinless case, but the analysis can be extended to the case in which spin is present.[4] Again we describe the three-momenta attached to a cluster "i" in a conventional "i" frame by $3N_i - 4$ internal variables V_i. (N_i is now the number of final particles attached to cluster "i"). There are now however two possible choices for "i" conventional frames, depending on whether cluster "i" is to the right or to the left of the z-pointing momentum transfer, i. e., whether Q_{hi} or Q_{ij} has only non-vanishing z-component. Calling these two frames i_r and i_l we have, in frame i_r

$$Q_{hi} = (0,\ 0,\ 0,\ \sqrt{-t_{hi}}),$$

and

$$Q_{ij} = (\sqrt{-t_{ij}}\ \sinh q_i\ ,\ 0,\ 0,\ \sqrt{-t_{ij}}\ \cosh q_i\ )\ ,$$

and in frame i_l

$$Q_{hi} = (-\sqrt{-t_{hi}}\ \sinh q_i\ ,\ 0,\ 0,\ \sqrt{-t_{hi}}\ \cosh q_i\ )$$

and

$$Q_{ij} = (0,\ 0,\ 0,\ \sqrt{-t_{ij}}).$$

It is clear that a boost of parameter q_i in the z direction transforms four-vectors from the frame i_l to i_r. Here q_i

can in general be thought of as an internal variable of cluster "i". If we define the invariant mass squared s_i of cluster "i" as

$$s_i = \left[\sum_{k=2}^{N_i+1} p_k \right]^2 , \qquad (2.4.1)$$

we have the relation

$$\sinh q_i = \frac{\lambda^{\frac{1}{2}}(t_{hi}, s_i, t_{ij})}{2\,(t_{hi}\, t_{ij})^{\frac{1}{2}}} \qquad (2.4.2)$$

where

$$\lambda(a, b, c) = a^2 + b^2 + c^2 - 2ab - 2bc - 2ac. \qquad (2.4.3)$$

If, however, $N_i = 1$, s_i becomes the mass squared of the outgoing particle attached to cluster "i", there are no V_i variables, and q_i is fixed by the values of the two adjacent momentum transfers t_{hi} and t_{ij}.

To complete the description of a process such as shown in Fig. 1, it is sufficient to give the relative orientation of each pair of consecutive conventional frames of the type h_l, i_r. In both these frames Q_{hi} is "diagonal", i. e., has vanishing time, x and y components, and again the relative orientation is specified by three parameters of the little group with respect to Q_{hi}, which we denote by g_{hi}. Thus we can express the amplitude as a function of the complete set of Toller variables

$$V_a \,,\; g_{ab} \,,\; t_{ab} \,,\; V_b \,, \ldots ,\; g_{yz} \,,\; t_{yz} \,,\; V_z \,.$$

It is easy to see that when an internal cluster "i" has only one outgoing particle, the amplitude ceases to depend separately on the two adjacent angles ν_{hi} and μ_{ij}, and depends only on the sum $\omega_i = \nu_{hi} + \mu_{ij}$. This is precisely the angle used in references 15) and 16) for the analysis of the case in which two Regge poles and three final particles are present.

In general we count the number of variables in the following way: there are $3N_i - 4$ internal variables for each cluster and four for each internal line (the invariant momentum transfer and three parameters of the little group). This gives a correct total of $3N - 4$, N being the total number of particles in the final state.

Up to now only one frame was associated to the end clusters. It is illustrative to introduce two additional frames a_r and z_l, in which p_{1a} and p_{1z} are respectively "diagonal", i. e., one of the initial particles is at rest (lab frames). These frames are again reached from the "neighbouring" frames a_l and z_r by boosts in the z direction of parameters q_a and q_z such that

$$\sinh q_a = \frac{s_a - m_{1a}^2 - t_{ab}}{2\, m_{1a}\, (-t_{ab})^{\frac{1}{2}}} \tag{2.4.4}$$

and

$$\sinh q_z = \frac{s_z - m_{1z} - t_{yz}}{2\, m_{1z}\, (-t_{yz})^{\frac{1}{2}}} .$$

Thus the lab energy of a given process described in term of Toller variables is just the energy developed by particle $1z$ when, starting from a frame in which it is at rest, undergoes the succession of Lorentz transformations of parameters

$$q_z\,,\; g_{yz}\,,\; q_y\,,\ldots,\; q_b\,,\; g_{ab}\,,\; q_a\,.$$

In the following we denote by $\cosh \eta$ this energy measured in units of the rest mass of the incident particle. The expression of $\cosh \eta$ in terms of the Toller variables is somewhat involved, and the leading term when all $\cosh \zeta_{ij}$ are large is

$$\cosh \eta \approx \cosh q_a \cosh \zeta_{ab} (\cosh q_b + \cos \omega_b) \cosh \zeta_{bc} \ldots (\cosh q_y + \cos \omega_y) \cosh \zeta_{yz} \cosh q_z\,. \tag{2.4.5}$$

3. MULTI - REGGE - POLE HYPOTHESIS

In terms of the Toller variables the multi-Regge-pole hypothesis reads[1)]

$$f(V_a, g_{ab}, t_{ab}, V_b, \ldots, V_y, g_{yz}, V_z) \xrightarrow[\text{all other variables fixed}]{\zeta_{ab}, \zeta_{bc}, \ldots, \zeta_{yz} \to \infty}$$

$$\phi_a(V_a, t_{ab}, \mu_{ab}) (\cosh \zeta_{ab})^{\alpha_{ab}(t_{ab})} \phi_b(\nu_{ab}, t_{ab}, V_b, t_{bc}, \mu_{bc})$$

$$\ldots (\cosh \zeta_{yz})^{\alpha_{yz}(t_{yz})} \phi_z(\nu_{yz}, t_{yz}, V_z). \qquad (3.1)$$

This expression is obtained by successive application of Toller's procedure for the expansion of a function on the unitary irreducible representations of the three-dimensional Lorentz group and extraction of the leading asymptotic contributions. At each step use is made of the factorization property of the residues of Regge poles. The dependence on the variables μ and ν , which also factorizes, has been incorporated in (3.1) in the residue functions.

It is important to remark that the limit in Eq. (3.1) cannot be achieved in a simple way in terms of other variables. For example, if one variable is chosen to be the total energy, a complicated prescription is required for the above limit.

4. CONSTRUCTION OF A MODEL

4.1 Basic Considerations

When the phase space integration is performed for the calculation of a cross section, from Eq. (3.1) it is clear that large values of those $\cosh \zeta_{ij}$ associated with high values of α_{ij} are favoured. As a consequence, distributions peaked at small values of the subenergies corresponding to lower lying

Regge trajectories are expected. An extreme example of this is Berger's calculation[20] of the process $\pi N \to \pi \rho N$ via double Regge exchange of a pion and a "Pomeranchon". The distribution that he obtains is strongly peaked at around 1.2 GeV. in the $\pi\rho$ subenergy. In general, if we adopt an a priori understanding that in this model an energy of approximately 2 GeV. is to be the rough dividing line between emission from a single vertex and emission from several vertices, we conclude that the inclusion of any trajectory below the Pomeranchuk would constitute double counting. That is to say, there is no increase with increasing lab energy of the average mass emitted from a pair of adjacent vertices connected by a non-Pomeranchuk trajectory. If there is a Pomeranchuk trajectory somewhere else in the chain, the available energy gets soaked up by the "Pomeranchons". Thus, the assumption of the existence of a Pomeranchuk Regge pole with factorizable residues is essential for our model.

The quantum numbers of particle combinations emitted at internal vertices must be those coupled to two "Pomeranchons", in particular $B = Y = I_z = 0$. Let us denote the average mass emitted from an internal vertex by m and assume that it may be approximated by a delta function centered at m. Evidently m cannot be less than $2\,m_\pi \approx .3$ GeV., while consistency of our model does not tolerate a value for m much greater than 2 GeV. Eventually we are going to allow this particle to decay into two or more particles. Correspondingly, we are going to represent by particles of masses m_{2a} and m_{2z} with various decay modes the outgoing particles attached to the end vertices. Of course, these particles must carry quantum numbers identical to those of the incident particles.

4.2 Differential Cross Sections

Under the above assumptions, and using the form of Eq. (3.1) for the amplitude, we arrive at the following expression for the differential cross section with n internal vertices

$$d\sigma^n_{az} = F_a(t_{ab})\, F_b(t_{ab}, \omega_b, t_{bc}) \dots F_z(t_{yz})\, (\cosh \zeta_{ab})^{\alpha_{ab}(t_{ab})} \dots$$

$$(\cosh \zeta_{yz})^{\alpha_{yz}(t_{yz})}\, \delta\!\left(\frac{p_{1a} \cdot p_{1z}}{m_{1a}\, m_{1z}} - \cosh \eta \right) dt_{ab} \dots dt_{yz}$$

$$d\omega_b \dots d\omega_y\, d(\cosh \zeta_{ab}) \dots d(\cosh \zeta_{yz}) \qquad (4.2.1)$$

4.3 Additional Assumptions

In order to make this model practicable, we have still to introduce the following specific assumptions:

a) An expression for the Pomeranchuk trajectory

b) Exponential dependence of the end vertex functions in the momentum transfer.

c) Also exponential dependence of the internal vertex functions in the adjacent momentum transfers. Independence of ω can be assumed until some better understanding on this point is achieved.

d) Equation (4.2.1) is to be integrated over all phase space. This implies using an asymptotic Regge pole expansion down to threshold. Recent work by Dolen, Horn and Schmid suggests that this may be a reasonable representation for the amplitude, at least in an average sense.[21] There are however numerical difficulties in performing this $3n + 2$ dimensional integration and in a first attempt we avoid them introducing some further approximations described in the next section.

e) Branching ratios for the different decay modes of the final particles. In the next section we give a particular example.

5. FURTHER DEVELOPMENT OF THE MODEL

5.1 Additional Approximations

We indicate here some additional approximations that make it possible to carry out the program outlined in the previous section without performing a detailed numerical integration of Eq. (4.2.1). The present calculation should be taken as a rough estimate and used only for the purpose of orientation and illustration of the model.

We start by substituting the exact expression for $\cosh \eta$ by the asymptotic one given by Eq. (2.4.5). We then define

$$x^{+}_{az}(\eta, n) = \ln \frac{\cosh \eta}{\cosh q_a \quad \cosh q_z \quad \prod_{i=b}^{y} (\cosh q_i + \cos \omega_i)} \qquad (5.1.1)$$

$$x_{ij} = \ln (\cosh \zeta_{ij}) , \qquad (5.1.2)$$

and we write, using again asymptotic approximations and a linear expression for the Pomeranchuk trajectory

$$d\sigma^{n}_{ab} \approx f_a(t_{ab}) \, f_z(t_{yz}) \prod_{i=b}^{y} f_i(t_{hi}, \omega_i, t_{ij})$$
$$\exp \left[2\alpha' \, (t_{ab} \, x_{ab} + \ldots + t_{yz} \, x_{yz}) \right] \, \delta(x_{ab} + \ldots + x_{yz} - x^{+})$$
$$dt_{ab} \ldots dt_{yz} \, dx_{ab} \ldots dx_{yz} \, d\omega_b \ldots d\omega_y \qquad (5.1.3)$$

The key simplification is to assume that for large $\cosh \eta$ the dependence of x^{+}_{az} on the t's and ω's , as given by Eq. (5.1.1), is sufficiently slow that we can replace the denominator on the right hand side by its value when all internal t's are set equal to some average value $-\Delta$, the end t's set equal to $-\Delta_a$ and $-\Delta_z$, and all $\cos \omega$'s set equal to some average, $\overline{\cos \omega}$.
Thus we replace Eq. (5.1.1) by

$$x^{+}_{az}(\eta, n) = \ln \frac{\cosh \eta}{\overline{\cosh q_a} \quad \overline{\cosh q_z}} - n \ln \lambda , \qquad (5.1.4)$$

where

$$\lambda = 1 + \frac{m^2}{2\Delta} + \overline{\cos\omega} . \qquad (5.1.5)$$

If $\Delta_a \ll m_{1a}^2$, as we expect if particle 1a is a nucleon, we have from Eq. (2.4.4)

$$\overline{\cosh q_a} \approx \begin{cases} 1 \text{ if } m_{2a} = m_{1a} \\ \dfrac{m_{2a}^2 - m_{1a}^2}{2 m_{1a} (\Delta_a)^{\frac{1}{2}}} \text{ if } m_{2a} \gg m_{1a} . \end{cases} \qquad (5.1.6)$$

The effect of approximation (5.1.4) is to decouple the integrations over the t's and the ω's from those over the x's . Assuming now

$$\int d\omega_i f(t_{hi}, \omega_i, t_{ij}) = g \exp\left[\gamma(t_{hi} + t_{ij})\right] , \qquad (5.1.7)$$

$$\begin{aligned} f_a(t_{ab}) &= g_a \exp(\gamma_a t_{ab}) , \text{ and} \\ f_z(t_{yz}) &= g_z \exp(\gamma_z t_{yz}) , \end{aligned} \qquad (5.1.8)$$

after performing the ω and t integrations in formula (5.1.3), letting the t's run from 0 to $-\infty$, we have

$$\sigma_{az}^n \approx \frac{g_a\, g_z\, g^n}{(\gamma_a+\gamma)(\gamma_z+\gamma)(2\gamma)^{n-1}} \int \cdots \int \frac{dx_{ab}}{1+y_{ab}x_{ab}} \cdots \frac{dx_{yz}}{1+y_{yz}x_{yz}}\, \delta\,(x_{ab}+ \dots + x_{yz} - x_{az}^{+}) \qquad (5.1.9)$$

where

$y_{ab} = 2\alpha'/(\gamma_a+\gamma)$, $y_{yz} = 2\alpha'/(\gamma_z+\gamma)$, and $y_{ij} = \alpha'/\gamma$,

with ij = bc, ... , xy .

For $n > 1$, the integrals in Eq. (5.1.9) must be performed numerically, but with $\gamma = \gamma_a = \gamma_z$ a substantial simplification occurs, leading to

$$\sigma^n_{az} = \frac{g_a\, g_z}{2\,\gamma\, n!}\left[\frac{g}{2\gamma}\quad x^+_{az}(\gamma,n)\right]^n \quad F_n(y \quad x^+_{az}(\gamma,n)) \qquad (5.1.10)$$

where $y = \alpha'/\gamma$,

$$F_0(z) = \frac{1}{1+z} \quad ,$$

$$F_{n+1}(z) = \frac{n+1}{z^{n+1}} \int_0^\infty \frac{z'^n\, F_n(z')}{1-z'+z}\, dz' \;.$$

Some properties of the functions $F_n(z)$ are

$$F_n(z) \underset{z \to 0}{\longrightarrow} 1 - z + O(z^2)$$

$$F_n(z) \underset{z \to \infty}{\longrightarrow} \frac{n!}{z^n}\,\frac{1+n}{1+n+z} \prod_{n'=1}^{n} \ln\,(1+z/n').$$

The latter form is actually a reasonable approximation in all the desired region of z for values of n up to 3 or 4 .

5.2 Application to p-p Collisions

Let us use Eq. (5.1.10) for the description of production processes in p-p collisions and review what parameters appear and what is their physical significance.

We want to consider two possibilities for particles 2a and 2z: each of them is either a proton or an $I = \frac{1}{2}$ isobar representing a whole family of possible physical states emitted at this vertex. Thus we define two parameters g_e and g^* such that

$$\frac{g_a}{(2\gamma)^{\frac{1}{2}}} \begin{cases} = g_e & \text{if particle 2a is a proton} \\ = g^* & \text{if particle 2a is an isobar.} \end{cases}$$

When particle 2a is an isobar, the value of $\overline{\cosh q_a}$ depends on the isobar mass and it constitutes a third parameter which we denote by $\cosh q^*$. Next we have λ and $g/2\gamma$; equations (5.1.5) and (5.1.7) show how they are related to the mass and coupling of the boson emitted at an internal vertex. Finally

y contains the dependence on the slope of the Pomeranchuk trajectory.

We have still to mention the decay schemes for the boson and the isobar produced in the collision. We assume that the first goes into two pions or two isospin-one dipions in proportions $\cos^2\theta$ and $\sin^2\theta$, whereas the second decays into πN and $\pi\Delta$ in fractions $\cos^2\theta^*$ and $\sin^2\theta^*$.

5.3 Results and Discussion

The scheme described above, in spite of its drastic assumptions, is able to provide a reasonable description for the trend and approximate values of the elastic and inelastic cross sections at currently available accelerator energies. In Table 1 we show

Table 1. Two sets of values of the parameters obtained by fitting p-p cross sections

	λ	$g/2\gamma y$	y	g_e	g^*	$\cosh q^*$	θ	θ^*
Set 1	1.90	1.21	.38	4.59	1.14	2	.91	.58
Set 2	2.14	1.12	.34	4.47	1.27	2	1.25	.32

two sets of values for the parameters: Set 1 is obtained by fitting the elastic cross section and the cross sections for production of given numbers of prongs. However, it predicts a cross section of 3.7 mb. for the $\pi^+\pi^-pp$ final state at 30 GeV/c. Because the experimental value seems to be rather 1 mb., the partial decays of the boson into two pions and of the isobar into $\pi\Delta$ were cut down to 10%. Thus in the second set θ and θ^* are fixed, and the value obtained for the $\pi^+\pi^-pp$ cross section at 30 GeV. is 1 mb. We see that the effect of this change on the other parameters is not very important. Because of technical reasons in neither fit was $\cosh q^*$ allowed to be larger than two. Higher values of this parameter, which show a tendency to improve the fit, would mean a higher value for the isobar mass, and this is still quite tolerable, as will be shown below.

In a recent fit of elastic p-p , π-p , and p-$\bar{p}$ data, Rarita et al.[22] have obtained values ranging from $1.77/\mathrm{GeV}^2$ to $3.25/\mathrm{GeV}^2$. for the coefficient of t in the exponential at a proton-proton-"Pomeranchon" vertex. If we choose for concreteness $\gamma = 2/\mathrm{GeV}^2$, from Table 1 and the relation $y = \alpha'/\gamma$ we obtain $\alpha' = .7/\mathrm{GeV}^2$, a value higher than obtained in ref. 22), but not beyond reason.

In the two Regge pole case, Chan et al. have shown examples in which ω is peaked around the value π.[16] If in Eq. (5.1.5) we take $\overline{\cos\omega} = -1$, and if we assume that the distribution in t is controlled by γ, i. e. $\Delta = 1/2\gamma$, we obtain from Table 1

$$m^2 \cong 2\Delta\lambda \cong 1\ \mathrm{GeV}^2.$$

This is a quite reasonable value for the average mass emitted at an intermediate vertex. Finally, from Eq. (5.1.6) we obtain for the isobar mass a value of approximately 1.7 GeV.

The effect of the values obtained for the different couplings is best shown by the results in Table 2, where the contributions of the various possible diagrams to the total cross section are given in detail for an incident momentum of 30 GeV/c.

Table 2. Cross sections in mb. contributed by different diagrams for p-p collisions at 30 GeV/c, with parameters of set 2.

Number of isobars \ Number of internal vertices	0	1	2	3
0	9.16	10.78	3.59	.23
1	5.81	5.30	1.01	.01
2	.94	.58	.03	.00

It is clear that with minor changes at the end vertices, the model can be used to describe collisions involving any pair of incident particles.

It is tempting to extrapolate and see what are the predictions of the model at extremely high energies with the parameters determined in the accelerator region. In refs. 18) and 2) it is shown that if the Pomeranchuk trajectory is flat, any amplitude with more than three Pomeranchuk lines violates the Froissart limit. In the present model a diagram with n internal vertices contributes to the cross section a term behaving like $(\ln(\ln s))^n/\ln s$ for large values of s (energy squared in the C. M. system). In the example given, the sum over all possible diagrams appears to behave like s raised to the power .16 in a region up to 10^6 GeV. This means for instance values of 55 mb. and 80 mb. for the total cross section at incident momenta of 300 GeV/c and 3000 GeV/c, respectively. Thus, there is an inconsistency in our model, because the elastic cross section in the forward direction divided by s has a constant behavior. This inconsistency is not surprising: it is pointed out in ref. 11) that violations of unitarity occur when cuts in the angular momentum plane are not included. Another weak point in our model is possibly related to the preceding one: the predicted average multiplicity increases too slowly. A typical value is 6.5 at 3000 GeV/c. It appears that a mechanism for suppressing the low multiplicities at high energy would improve both the behavior of the total cross section and of the average multiplicity.

Up to now we have concentrated on total cross sections. It is of course possible to look at distributions in different variables. We believe for example that the exponential distribution in transverse components of the momenta will follow from the assumed exponential behavior of the vertex functions in the invariant momentum transfers.

6. CONCLUSION

The results presented here are just the beginning of our developing a quantitative understanding of production processes in terms of a multi-Regge analysis. Still there is much to be done. We have to correct some extremely crude approximations and to incorporate new pieces of experimental evidence. We want to end by encouraging the experimental study and detailed analysis of the type of processes considered here. We believe that it is a rich field to exploit and that the results obtained up to now are encouraging.

References

1) N. F. Bali, G. F. Chew and A. Pignotti, UCRL-17530, to be published in Phys. Rev.
2) N. F. Bali, G. F. Chew and A. Pignotti, Phys. Rev. Letters 19, 614 (1967).
3) T. W. B. Kibble, Phys. Rev. 131, 2282 (1963).
4) K. A. Ter-Martirosyan, Soviet Phys. JETP 44, 341 (1963).
5) A. M. Popova and K. A. Ter-Martirosyan, Nuclear Phys. 60, 107 (1964).
6) Z. Koba, Fortschritte der Physik 11, 118 (1963).
7) I. G. Ivanter, A. M. Popova and K. A. Ter-Martirosyan, Soviet Phys. JETP 19, 387 (1964).
8) K. A. Ter-Martirosyan, Nuclear Phys. 68, 591 (1964).
9) M. S. K. Razmi, Nuovo Cimento 31, 615 (1964).
10) I. A. Verdiev, A. M. Popova and K. A. Ter-Martirosyan, Soviet Phys. JETP 19, 878 (1964).
11) I. A. Verdiev, O. V. Kancheli, S. G. Matinyan, A. M. Popova and K. A. Ter-Martirosyan, Soviet Physics JETP 19, 1148 (1964).
12) J. Joseph and H. Pilkuhn, Nuovo Cimento 33, 1407 (1964).
13) J. C. Polkinghorne, Nuovo Cimento 36, 857 (1965).
14) G. M. Fraser and R. G. Roberts, Nuovo Cimento 47, 339 (1967).
15) H. M. Chan, K. Kajantie and G. Ranft, Nuovo Cimento 49, 157 (1967).
16) H. M. Chan, K. Kajantie, G. Ranft, W. Beusch and E. Flaminio, Nuovo Cimento 51, 696 (1967).
17) F. Zachariasen and G. Zweig, Phys. Rev. 160, 1322 (1967), and Phys. Rev. 162, 1326 (1967).
18) K. Kajantie, CERN TH. [illegible], preprint.
19) M. Toller, Nuovo Cimento 37, 631 (1965).
20) [illegible] L. Berger, UCRL-[illegible], preprint.
21) R. Dolen, D. Horn and C. Schmid, CALT-68-143, preprint.
22) W. Rarita, R. Riddell, C. Chiu and R. Phillips, UCRL-17523,